



# Investigation into Benefits of Coupling a Frame Structure with a Rocking Rigid Block

Stefano Pagliaro<sup>(✉)</sup>, Angelo Aloisio, Angelo Di Egidio<sup>(✉)</sup>, and Rocco Alaggio

Department of Civil, Architectural-Construction and Environmental Engineering,  
University of L'Aquila, L'Aquila, Italy

{stefano.pagliaro,angelo.aloisio1}@graduate.univaq.it,  
{angelo.diegidio,rocco.alaggio}@univaq.it

**Abstract.** This paper analyses the linear elastic coupling of a frame structure and a rigid block aimed at improving the dynamic behaviour of the frame. A multi-storey frame structure, modelled as a two-degree of freedom linear system, is connected by an elastic device to a rigid block. The nonlinear equations of motion of the coupled-system are obtained by a Lagrangian approach and successively numerically integrated to analyse the behaviour of the coupled system. Simulations are performed using harmonic excitation as forcing term. The results are summarized in gain maps. The maps show the ratio between the maximum displacements or drifts of the coupled and uncoupled systems in the plane of the system's parameters. The results of the numerical simulations show that there are wide regions of the parameters where the coupling may be effective. Experimental simulations are then performed to verify the actual effectiveness of such a coupling. A scaled shear-type 2 d.o.f frame coupled with an aluminium rigid block is sinusoidally forced by an electro-dynamic long-stroke shaker. The system's response in terms of displacements is measured by no-contact optical/laser sensors. The experimental tests confirm the effectiveness of the coupling as expected by the analytical model.

**Keywords:** Visco-elastic coupling · Rocking rigid block · Gain coefficients and maps · Experimental investigation

## 1 Introduction

After the pioneering work [1] that examined the stability of a standalone slender block subject to a base motion, several papers analysed the dynamics of rigid blocks. Both the seismic excitation [2,3] and other kinds of ground excitation, such as harmonic or impulsive one-sine excitation were considered in [4–6]. A general formulation for the rocking and slide-rocking motions of freestanding symmetric rigid blocks is proposed in [7,8]. Three-dimensional blocks were studied in [9,10], whereas other papers investigated the dynamics of rigid blocks in a general way as in [11].

In recent years many studies have regarded the coupling of rigid block with other mechanical system in order to protect the block from overturning. An example is the use of base anchorages [12, 13]. Other examples are [14, 15] where the efficiency of the base isolated system was studied. A mass-damper dynamic absorber in the shape of a pendulum was used by different authors [16–19], who demonstrated the general effectiveness of this kind of protection device. Instead, in [20–22] a mass-damper modelled as a single degree of freedom and running on the top of the block was considered as safety device. Not only passive, but also active or semi-active devices were used to improve the dynamic and seismic performances of blocks. For example [23] studied the use of semi-active anchorages using feedback-feedforward strategies to increase the acceleration required to topple a reference block. Papers [24] and [25] used an active control technique based on the Pole Placement method to increase the amplitude of the base excitation able to topple a rigid block.

It is not frequent the use of rocking rigid block as protecting device of other kinds of structures. Recently some authors have considered a rigid coupling between a frame and a rocking wall, in order to improve the seismic behaviour of the frame [26]. Instead, in [27], the visco-elastic coupling of a frame structure and a rigid block aimed at improving the dynamic behaviour of the frame is studied under harmonic excitation.

This paper analyses the behaviour of a 2 d.o.f. shear-type frame structure coupled with rigid block both theoretically and experimentally. An elastic device connects the block to the structure. The nonlinear equations of motion of the coupled-system are obtained by a Lagrangian approach, then they are numerically integrated to investigate the response of the coupled system. A parametric analysis is performed and the results summarized in a behaviour map. It shows the ratio between the maximum displacements or the drifts of the coupled and uncoupled systems in the plane of the system's parameters. Such map allows an immediate understanding of the effects of the block that has a beneficial effect when the ratio of the displacements is less than unity. Experimental simulations are performed to verify the effectiveness of such a coupling. A scaled shear-type 2 d.o.f frame elastically coupled with an aluminium rigid block is harmonically driven by an electro-dynamic long-stroke shaker. The system's response, in terms of displacements, measured by no-contact and optical/laser sensors, is post-processed by means of the software MATLAB<sup>®</sup> and Mathematica<sup>®</sup>. Then, both experimental and theoretical results are compared.

## 2 Motivations of the Study

Frame structures can be coupled with other mechanical systems (i.e., mechanical devices or other structures) to improve their behaviour under external loads. Some examples of such mechanical systems are oscillating masses working as tuned mass dampers, dynamic mass absorbers and elasto-plastic dampers. Among others possibilities, a rocking rigid block can be used to improve the dynamic and seismic behaviour of a frame structure. For example, the authors in [26] consider a rigid coupling between a frame and a rocking wall that has the same height of the frame.

This paper considers a non-rigid connection between the frame and the block. Figure 1 shows a scheme of the coupled mechanical system. The block can be shorter than the frame. In the presented model the connection between the block and the frame is at the first storey, the lowest one. The paper aims at investigating the possibility to improve the dynamics of the structure standing above the connection point by means of an external rocking block.

It is implicitly assumed that a two-degree of freedom linear system can be used as model for a multi-storey frame structure as in [28, 29].

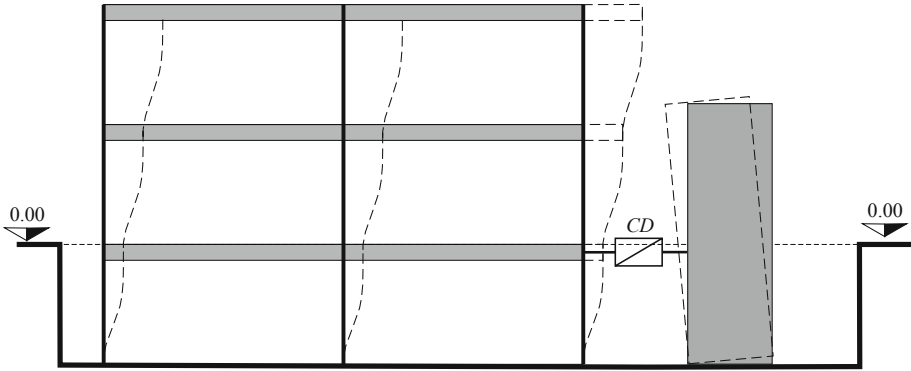


**Fig. 1.** Coupling between a frame structure and the rocking wall (CD: Coupling Device).

### 3 Mechanical Model of the Experimented System

A scaled shear-type 2 d.o.f frame is coupled with a rocking rigid block by means of a linear elastic device, which connects the first storey of the frame to a point on the vertical side of the block. The block has a mass  $M = \rho \times 2b \times 2h_b \times s$ , where  $\rho = 2450 \text{ kg/m}^3$  (aluminium) and  $s$  is the dimension orthogonal to the plane of the figure. Figure 2 shows the geometrical configuration and characteristics of the coupled mechanical system.

#### 3.1 Equations of Motion

It is assumed that the block cannot slide, therefore only rocking motions can occur. Consequently, three Lagrangian parameters fully describe the motion. Such parameters are the displacements (relative to the ground) of the two d.o.f. system  $u_1$  and  $u_2$ , and the rotation of the block  $\vartheta$ . Figure 2b shows the positive directions of the three Lagrangian parameters. Two sets of three equations of motion, which describe the motion of the system when the block rocks around either the left corner  $A$  or the right corner  $B$ , have to be obtained. For the sake

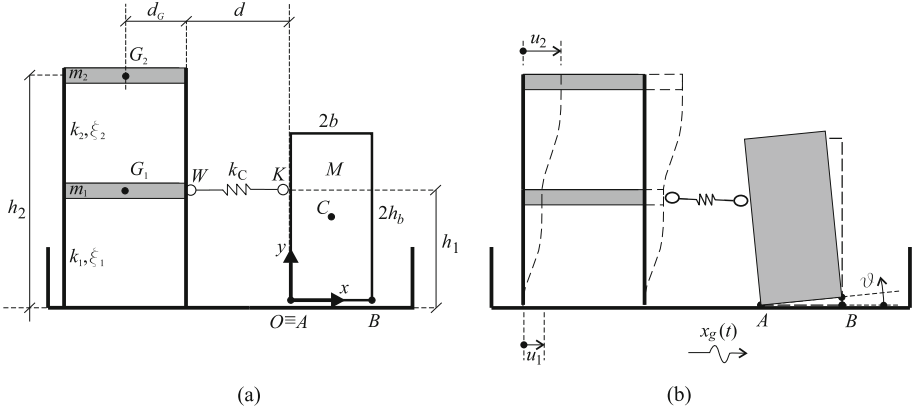


**Fig. 2.** Mechanical system: (a) geometrical characterization of the system; (b) Lagrangian parameters (positive directions).

of brevity, in this section, only the relationships needed to describe the motion of the system, when the block is rocking around the left corner  $A$  are reported.

The positions of the mass centres of the bodies are evaluated with respect to an inertial reference frame with origin in  $O$ , initially coincident with the left base corner  $A$  of the block (Fig. 2a). The positions of the mass centres  $G_1$  and  $G_2$  of the two d.o.f. structure are:

$$\mathbf{x}_{G1}(t) = \begin{Bmatrix} x_g(t) - d - d_G + u_1(t) \\ h_1 \\ 0 \end{Bmatrix}; \quad \mathbf{x}_{G2}(t) = \begin{Bmatrix} x_g(t) - d - d_G + u_2(t) \\ h_2 \\ 0 \end{Bmatrix} \quad (1)$$

The position of the mass center  $C$  of the block during a rocking around the left corner  $A$  reads:

$$\mathbf{x}_C(t) = \begin{Bmatrix} x_g(t) \\ 0 \\ 0 \end{Bmatrix} + \begin{bmatrix} \text{Cos}\vartheta(t) & -\text{Sin}\vartheta(t) & 0 \\ \text{Sin}\vartheta(t) & \text{Cos}\vartheta(t) & 0 \\ 0 & 0 & 1 \end{bmatrix} \begin{Bmatrix} b \\ h_b \\ 0 \end{Bmatrix} \quad (2)$$

where the matrix is the rotation tensor of the block. The kinetic energy of the mechanical system during a rocking motion of the block around the left corner  $A$  reads:

$$T = \frac{1}{2} \left[ \sum_{i=1}^2 m_i (\dot{\mathbf{x}}_{Gi}(t) \cdot \dot{\mathbf{x}}_{Gi}(t)) + J_C (\dot{\theta}(t) \cdot \dot{\theta}(t)) + M (\dot{\mathbf{x}}_C(t) \cdot \dot{\mathbf{x}}_C(t)) \right] \quad (3)$$

where  $m_1$  and  $m_2$  are the masses of the 2 d.o.f. system;  $\dot{\theta}(t) = \{0, 0, \dot{\vartheta}(t)\}^T$  and  $J_C$  is the polar inertia of the block with respect to its center of mass.

In order to evaluate the potential energy for a rocking motion around the corner  $A$ , the distance vector between the couple of points  $W$ ,  $K$  has to be evaluated. It is required to compute the potential energy associated to the elastic device with stiffness  $k_C$ . Such a distance vector reads:

$$\mathbf{x}_{WK}(t) = \mathbf{x}_K(t) - \mathbf{x}_W(t) = \begin{Bmatrix} d - \text{Sin}\vartheta(t)h_1 - u_1(t) \\ -h_1 + \text{Cos}\vartheta(t)h_1 \\ 0 \end{Bmatrix} \quad (4)$$

The potential energy of the system then reads

$$V = [Mg(\mathbf{x}_C(t) - \bar{\mathbf{x}}_C) \cdot \mathbf{j}] + \frac{1}{2} \left[ k_1 u_1(t)^2 + k_2 (u_2(t) - u_1(t))^2 \right] + \frac{1}{2} \left[ k_C \left( \sqrt{\mathbf{x}_{WK}(t) \cdot \mathbf{x}_{WK}(t)} - d \right)^2 \right] \quad (5)$$

where  $k_1$  and  $k_2$  are the stiffness of the 2 d.o.f. system;  $g$  is the gravity acceleration;  $\mathbf{j} = \{0, 1, 0\}^T$  is the unity vector of the  $y$ -axis;  $\bar{\mathbf{x}}_C = \{b, h_b, 0\}^T$  is the positions of the mass center corresponding to the minimum potential energy of the system. Since  $\bar{\mathbf{x}}_C$  in Eq. 5 is constant, it consequently plays no role in the derivation of the equations of motion.

The damping of the 2 d.o.f. system is modelled through two linear viscous dashpots with damping coefficients  $c_1$  and  $c_2$ . The virtual work  $\partial W$  of the non-conservative viscous forces has to be considered to obtain the Lagrangian equations of motion; it reads

$$\partial W = -[c_1 \dot{u}_1(t) \delta u_1(t) + c_2 (\dot{u}_2(t) - \dot{u}_1(t)) (\delta u_2(t) - \delta u_1(t))] \quad (6)$$

Finally, the equation of motion can be obtained by:

$$\left[ \frac{d}{dt} \left( \frac{\partial L}{\partial \dot{q}_i} \right) - \frac{\partial L}{\partial q_i} \right] \delta q_i = \delta W(\delta q_i), \quad \forall \delta q_i \neq 0; (i = 1, 2, 3) \quad (7)$$

where  $L = T - V$  is the Lagrangian function,  $(q_1, q_2, q_3) = (u_1, u_2, \vartheta)$  and  $(\delta q_1, \delta q_2, \delta q_3) = (\delta u_1, \delta u_2, \delta \vartheta)$ . The equations of motion then read:

$$\begin{aligned} -k_C (d - h_1 \sin \theta - u_1) \frac{(\sqrt{d^2 - 2(d-u_1)h_1 \sin \theta - 2du_1 - 2h_1^2 \cos \theta + 2h_1^2 + u_1^2} - d)}{\sqrt{d^2 - 2(d-u_1)h_1 \sin \theta - 2du_1 - 2h_1^2 \cos \theta + 2h_1^2 + u_1^2}} \\ + (c_1 + c_2) \dot{u}_1 - c_2 \dot{u}_2 + (k_1 + k_2) u_1 - k_2 u_2 + m_1 (\ddot{x}_g + \ddot{u}_1) = 0 \\ \hline c_2 (\dot{u}_2 - \dot{u}_1) + k_2 (u_2 - u_1) + m_2 (\ddot{x}_g + \ddot{u}_2) = 0 \\ \hline J_A \ddot{\theta} + \cos \theta (bgM - h_b M \ddot{x}_g) - M \sin \theta (b \ddot{x}_g + g h_b) + \\ k_C h_1 ((u_1 - d) \cos \theta + h_1 \sin \theta) \frac{(\sqrt{d^2 - 2(d-u_1)h_1 \sin \theta - 2du_1 - 2h_1^2 \cos \theta + 2h_1^2 + u_1^2} - d)}{\sqrt{d^2 - 2(d-u_1)h_1 \sin \theta - 2du_1 - 2h_1^2 \cos \theta + 2h_1^2 + u_1^2}} = 0 \end{aligned} \quad (8)$$

where  $J_A$  is the polar inertia of the block with respect to the right base corner  $A$  and the dependence on time  $t$  is removed to make the equation more readable. The equations of motion referring to a block that rocks around the right corner  $B$  can be obtained similarly.

### 3.2 Uplift and Impact Conditions of the Block

The uplift of the block around point  $A$  takes place when the resisting moment  $M_R = Mgb$ , due to the weight of the block gets smaller than the overturning moment  $M_O = -M\ddot{x}_g(t)h_b + [k_C u_1(t)]h_1$  due to the inertial force and to the elastic one of the internal coupling device. All these moments are evaluated with respect to the base point  $A$  (Fig. 2a). By vanishing the sum of the two previous moments, it is possible to obtain the external acceleration  $\ddot{x}_g$  able to uplift the block. Such an acceleration reads:

$$\ddot{x}_g = \frac{g}{\lambda} + \frac{k_C u_1(t)h_1}{Mh_b} \quad (9)$$

where  $\lambda = h_b/b$  is the slenderness of the block. In absence of the coupling with the device, the uplift condition is the same of a stand-alone block.

During the rocking motion, when the rotation  $\vartheta(t)$  approaches zero, an impact between the block and the ground occurs. Post-impact conditions of the rocking motion can be found assuming that the impact happens instantly, the body position remains unchanged and the angular momentum is maintained. The post-impact angular velocity is equal to  $\vartheta^+ = \eta r \vartheta^-$ , where  $r = (J_O - 2b S_y)/J_O$  is the restitution coefficient equal to that of stand-alone blocks ( $J_O$  is the polar inertia of the block with respect to one of the two base corners;  $S_y = Mb$  is the static moment of the block with respect to a vertical axis passing through one of the two base corners);  $\eta$  is a coefficient less than unity, introduced to include a further loss of mechanical energy. Such a coefficient has been experimentally determined by identifying several experimental and numerical free rocking motions. The analysis has provided the value  $\eta = 0.978$ .

## 4 Parametric Analysis

A parametric analysis is performed to investigate the behaviour of the coupled system by numerically integrating the equations of motion. The parameters considered in this analysis are the circular frequency of the harmonic excitation  $\Omega$  and the coupling stiffness  $k_C = \beta k_1$ .

The harmonic excitation used in the analyses is  $\ddot{x}_g(t) = A_s \sin(\Omega t)$ ,  $0 \leq t \leq t_{\max}$ , where  $A_s$  is the amplitude of the harmonic excitation and  $t_{\max}$  is the maximum time used in the numerical integrations ( $t_{\max} = 120$  s). The comparison among numerical and experimental results is performed in stationary conditions, after that the transient dynamics is vanished due to the damping of the system. Since the mechanical system is nonlinear, its behaviour depends on the amplitude  $A_s$  of the excitation. A fixed value of the amplitude is taken  $A_s = 1.01g/\lambda$ , which is slightly greater than the uplift value of the stand-alone block.

#### 4.1 Frame and Block Characteristics

Both the numerical and the experimental analyses are performed on a scaled 2 d.o.f. model. With reference to Fig. 2, the geometrical characteristics of the mechanical system are shown in Table 1, whereas the mechanical characteristics of the system are shown in Table 2.

**Table 1.** Characteristics of the block.

Storeis	$2b$ (m)	$h_1$ (m)	$h_2$ (m)	$h_b$ (m)	$s$ (m)
2	0.05	0.2	0.496	0.2	0.10

**Table 2.** Characteristics of the 2 d.o.f. frame.

$k_1$ (N/m)	$k_2$ (N/m)	$m_1$ (kg)	$m_2$ (kg)	$\xi_1$	$\xi_2$
213.44	56.45	1.062	1.062	0.010	0.035

In Table 2,  $\xi_1$  and  $\xi_2$  are the damping ratios of the 2 d.o.f. shear-type frame. All the quantities in Table 2 are directly measured ( $m_1$  and  $m_2$ ) or identified through preliminary free motion of the uncoupled frame ( $k_1, k_2, \xi_1$  and  $\xi_2$ ).

#### 4.2 Gain Coefficients

The displacement  $u_1$  and the drift  $u_2 - u_1$  are used as indicators to evaluate the dynamic performance of the system. The smaller  $u_1$  and  $u_2 - u_1$  are, the greater the effectiveness of the coupling with the block is. As done in [28], two gain parameters are then introduced:

$$\alpha_1 = \frac{\max |u_1(t)|}{\max |\tilde{u}_1(t)|}, \quad \alpha_2 = \frac{\max |u_2(t) - u_1(t)|}{\max |\tilde{u}_2(t) - \tilde{u}_1(t)|} \quad (10)$$

where the displacements  $\tilde{u}_1$  and  $\tilde{u}_2$  refer to the uncoupled frame structure. If the parameters of Eq. 10 are less than unity, the coupling between the frame structure and the rocking block is beneficial for the frame structure. This paper aims to study the effects of the coupling on the part of the structure standing above the connecting point with the block (super-structure), therefore only  $\alpha_2$  is evaluated. The parametric analysis provides the gain map that represents the values of  $\alpha_2$  in a specific parameters plane.

#### 4.3 Gain Map

The gain map is the contour plot of the gain coefficient  $\alpha_2$ . The parameters are the circular frequency of the harmonic excitation  $\Omega$  and the stiffness ratio  $\beta$  of the coupling device.

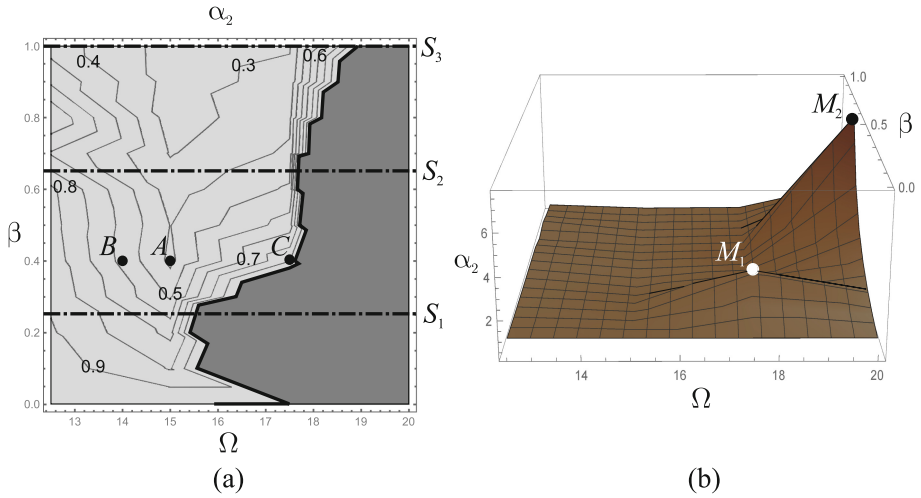


**Fig. 3.** Evaluation of the effectiveness of the coupling: (a) gain map of the coefficient  $\alpha_2$ ; (b) gain surface of the coefficient  $\alpha_2$ .

In Fig. 3a the gain map of the coefficient  $\alpha_2$  is shown. Inside the light grey region,  $\alpha_2$  is less than unity. Hence, this region, which is named gain region, represents combinations of the parameters for which the coupling with the rigid block is beneficial for the structure. In particular a minimum value of the coefficient  $\alpha_2 = 0.3$  can be reached. This means that a 70% reduction of the drift of the coupled system with respect to the drift of the uncoupled system can be achieved. Inside the dark grey region the coefficient  $\alpha_2$  is greater than unity and no advantage from the coupling occurs. As can be observed in Fig. 3b, the gain surface (whose projection on  $\Omega - \beta$  plane is the gain map of Fig. 3a) presents two relative maxima in points  $M_1$  and  $M_2$ . They are located in the dark grey region and correspond to resonance conditions between the harmonic frequency and the frequency of the first coupled mode of the linearised system. Even if the system is nonlinear, the smallness of the rocking angle during the motion makes its behaviour very close to that of a linear system. In the first coupled mode of the linearised system the frame lower storey and the block move in phase, thus causing a worsening of the behaviour of the coupled system with respect to that of the uncoupled one (see [27]).

In order to investigate how the coupling works, the time-histories of coupled and uncoupled system are analysed. Figure 4 shows the time evolution of the drift  $u_2 - u_1$  of both coupled and uncoupled system (left graphs) and of the displacement  $u_1$  and the angle  $\vartheta$  (right graphs). Both graphs in Fig. 4a refer to the point A in Fig. 3a, which is located in a relative minimum point of the  $\alpha_2$  gain surface. As can be observed, the time-history of the drift of the coupled system has a maximum amplitude smaller than the drift of the uncoupled system. Very interesting is the observation in the same graph of the time-histories of the



displacement  $u_1$  of the coupling storey and of the rocking angle  $\vartheta$ . By taking into account the positive directions of the Lagrangian parameters (see Fig. 2b), the first storey and the block move almost in counter-phase. In such a case the block works as a Tuned Mass Damper for the structure. The time-histories of the point  $B$  (Fig. 4b), located in a point of the map where  $\alpha_2$  is greater than that in the point  $A$ , show a smaller reduction of the coupled drift than the uncoupled one. The observation of the evolution of  $u_1$  and of  $\vartheta$  highlights the fact that the first storey and the block does not move in counter-phase, but neither in phase. As a consequence, there is a lower ability of the block to reduce the drift of the structure than the previous case. The time-histories of the point  $C$  (Fig. 4c), that is located very close to boundary of the gain region of the map in Fig. 3a (where  $\alpha_2 = 1$ ), show a further worsening of the effectiveness of the coupling. In fact, the maximum amplitude of the drifts of the coupled and of the uncoupled systems are almost the same. On the contrary, the evolution of  $u_1$  and  $\vartheta$  show that in this case the first storey and the block move almost in phase, thus vanishing the effect of the coupling.

## 5 Experimental Tests

The experimental investigation has been performed in the laboratory *Analytical, Numerical, Experimental Models for Civil Engineering* (ANEMCE), which is a section of the Dynamics Laboratory of the Department of Civil, Architectural-Construction and Environmental Engineering (DICEAA) at University of L'Aquila, Italy,

### 5.1 Experimental Setup

A number of challenging tasks have to be tackled in designing the experimental apparatus, aiming to a reliable investigation of the frame-rigid block nonlinear behaviour. Concerning the system under test, the rigid block is supported by an adjustable base (Fig. 5c), sliding over two guides anchored to the base of the frame. The movable base is equipped with two sharp-edged profiles, which allow the block to rock without sliding. The coupling spring is inserted in a thin rod, equipped with a hook on one side, avoiding instability of the spring under compression; The hooked end is locked with a catch on the first storey of the frame, while, on the other side, the rod is free to slide inside a flared hole, made in the block's centre of mass (Fig. 5a). The spring is fixed on both the hook and the rigid block (Fig. 5b).

Concerning the experimental setup (Fig. 5d), the frame's base is anchored to a wheeled support, pushed by an electrodynamic shaker, which is driven via a power control unit (amplifier) and a function generator having a controllable frequency and gain. Two high-resolution Laser sensors (Micro-Epsilon optoNCDT 1420) are used as contact-free devices for tracking the displacements of the two storeys. Measurements, observed via an oscilloscope and a spectrum analyser, are acquired by a digital computer data acquisition system storing real

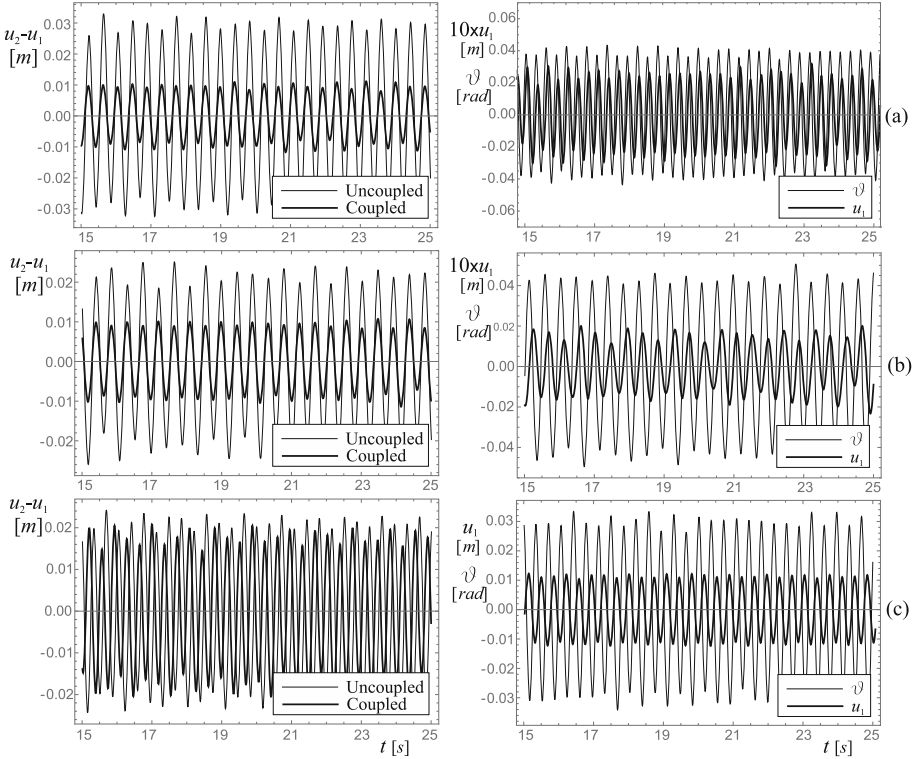


**Fig. 4.** Time-histories of the coupled and uncoupled system: (a) characteristics labelled with *A* in Fig. 3a ( $\Omega = 15; \beta = 0.4$ ); (b) characteristics labelled with *B* in Fig. 3a ( $\Omega = 14; \beta = 0.4$ ); (c) characteristics labelled with *C* in Fig. 3a ( $\Omega = 17.5; \beta = 0.4$ )

time outputs at the sampling interval of  $1/400$  s. A filter unit is implemented to cut off high frequencies induced by some overall noise. The recorded response is post-processed by means of the software MATLAB<sup>®</sup> and Mathematica<sup>®</sup>.

### 5.2 Gain Spectra

Gain spectra provide the gain coefficients  $\alpha_1$  or  $\alpha_2$  versus the frequency of the harmonic excitation. They formally are sections of the gain map (or of the gain surface), shown in Fig. 3. In the following section the interest will be focused on the sole  $\alpha_2$  gain spectrum.

Three experimental tests were performed, considering three different values of the coupling stiffness  $k_C$  (*i.e.* three values of  $\beta$ ), in order to obtain three different gain spectra. The experimental results are compared with three corresponding sections of the gain map, labelled with *S1*, *S2* and *S3* in Fig. 3. In order to obtain the experimental gain spectra, four different frequencies are considered for each value of the coupling stiffness; specifically  $\Omega = 12.5, 15.0, 17.5$  and  $20.0$  rad/s are

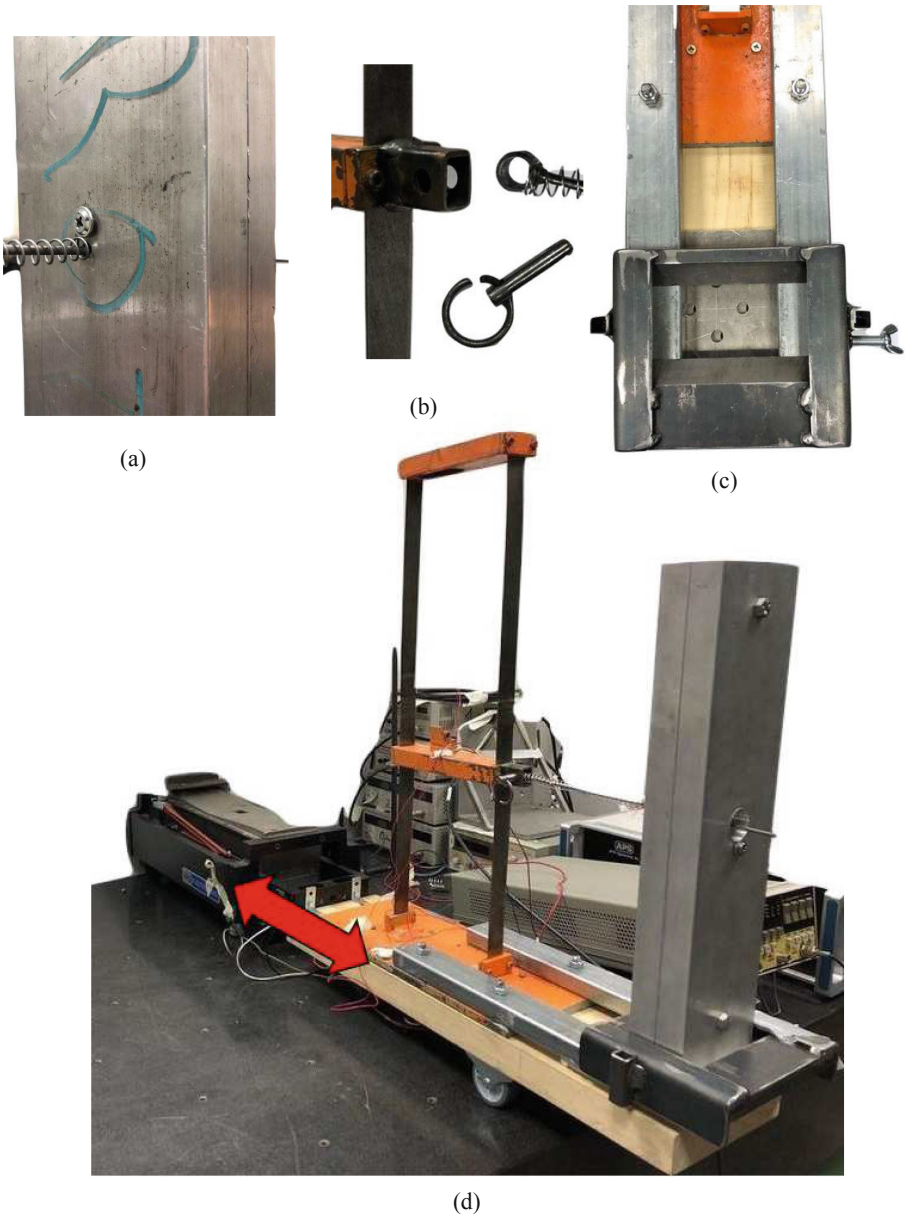


**Fig. 5.** Details of the structure under test; (a) connection between the block and the spring (the spring is held by the head of a screw inserted in the rigid block); (b) connection between the first storey and the rigid block; (c) adjustable base, sliding over two guides anchored to the base of the frame; (d) an overall view of the experimental setup.

considered. During the tests, the time-histories of the total displacements  $u_1$  and  $u_2$  of both coupled and uncoupled system are acquired. The  $\alpha_2$  gain coefficient is the ratio of the drifts  $u_2 - u_1$  of the coupled and uncoupled system.

Figure 6 shows three gain spectra, each one referring to different stiffness ratios  $\beta$ . Two different curves are reported in each graph. Solid line represents the gain spectrum obtained by the numerical integration of the mathematical model, whereas dashed line represents the gain spectrum obtained by the experimental investigation. It is useful remarking that the numerical curves (solid line) are section of the gain map in Fig. 3. Specifically, section  $S1$  refers to  $\beta = 0.25$ , section  $S2$  refers to  $\beta = 0.64$ , whereas section  $S3$  is obtained for  $\beta = 0.97$ .

The gain regions in each spectrum (the regions below the reference dash-dotted line passing through unity) are well described by the experimental results, since they are sufficiently close to the numerical curves. However, outside the gain regions, the numerical results show a faster growth than the experimental ones. For example, the numerical spectrum obtained for  $\beta = 0.25$  (upper left graph) has a maximum at about  $\Omega = 18.5$ . On the contrary, the experimental spectrum does not have a maximum in the range of the investigated frequency. This maximum value may correspond to the resonance condition between the frequency of the excitation and the frequency of the first linearised coupled mode, where the block and the first storey of the frame move in phase. Hence, the advantage from coupling vanishes and the gain coefficient  $\alpha_2$  is maximum.

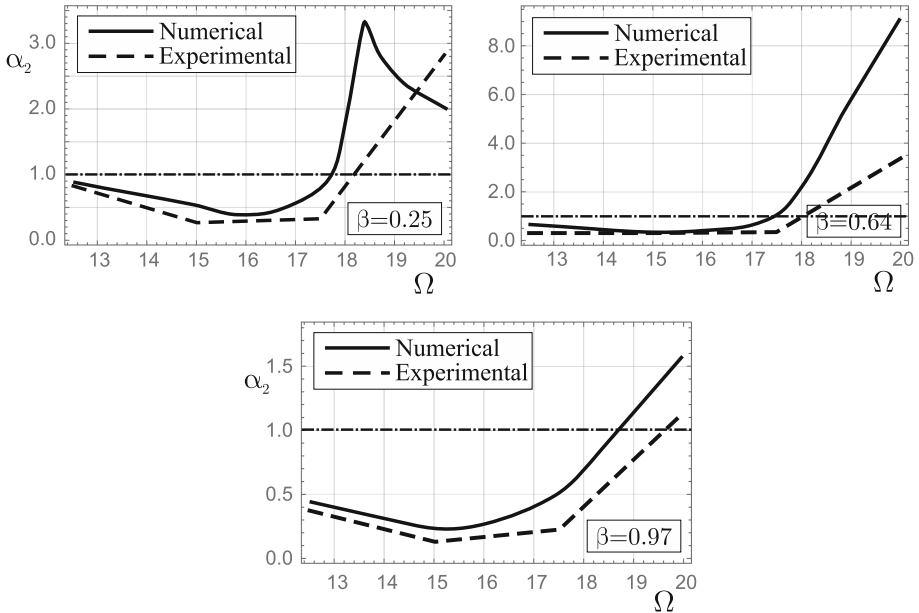


**Fig. 6.** Gain coefficient spectra are obtained for three different values of  $\beta$ . Continuous line represents the gain coefficient obtained from the analytical model and the dashed line represents the gain coefficient obtained from the experimental data.

In the other graphs, the numerical spectrum never reaches the resonance condition, since it is located outside the range of the considered frequencies  $\Omega$ . On the contrary, the experimental spectra never show a maximum inside the investigated frequencies. The growth that they manifest outside the advantage region is slower than the numerical curves. This fact is possibly related to differences among the real and numerical frequencies of the first linearised mode, mainly due to imperfections of the real system. The friction among helical springs and rod, the small planarity defect of the impacting surface of the block, the not perfect symmetry of the block, shift the frequency of the first linearised coupled mode, outside the investigated window.

## 6 Conclusions

A 2 d.o.f. shear-type system is elastically coupled with an aluminum rocking block to improve the dynamics of the frame. The nonlinear equations of motion were obtained by a Lagrangian approach and successively numerically integrated to analyze the behavior of the coupled system. The coupling with the block was considered beneficial for the frame structure when there is a reduction in the displacements of the structure. Simulations were performed considering a harmonic excitation. The results were summarized in a gain map plotted in the system's parameters plane. The characterizing parameters are the frequency of the harmonic excitation and the stiffness of the coupling device. The gain map provides the ratio of the maximum drift of the coupled and of the uncoupled systems. When this ratio is less than unity the coupling with the block improves the dynamics of the frame structure. Results have shown the existence of a large advantage region in the parameters plane, where the coupling is beneficial for the system.

Experimental simulations were performed to verify the effectiveness of the frame-block coupling. The same mechanical system, investigated in numerical simulations, was experimentally tested by means of a harmonically driven electro-dynamic long-stroke shaker. The response of the experimental system, arranged in gain spectra (i.e. sections of the previous gain map), were compared with the numerical sections. The comparison confirms the rightness of the analytical model in predicting the actual behaviour of the experimental system. Moreover, it gives an attestation of the capability of rocking rigid blocks in improving the response of a linear frame system.

## References

1. Housner, G.W.: The behavior of inverted pendulum structures during earthquakes. *Bull. Seismol. Soc. Am.* **53**(2), 404–417 (1963)
2. Taniguchi, T.: Non-linear response analyses of rectangular rigid bodies subjected to horizontal and vertical ground motion. *Earthq. Eng. Struct. Dyn.* **31**, 1481–1500 (2002)

3. Psycharis, I.N., Fragiadakis, M., Stefanou, I.: Seismic reliability assessment of classical columns subjected to near-fault ground motions. *Earthq. Eng. Struct. Dyn.* **42**(14), 2061–2079 (2013)
4. Spanos, P., Koh, A.: Rocking of rigid blocks due to harmonic shaking. *J. Eng. Mech.* **110**, 1627–1642 (1984)
5. Kounadis, A.N.: Parametric study in rocking instability of a rigid block under harmonic ground pulse: a unified approach. *Soil Dyn. Earthq. Eng.* **45**, 125–143 (2013)
6. Vassilios, M., Mackie, K.R., Stojadinović, B.: Dynamic response analysis of solitary flexible rocking bodies: modeling and behavior under pulse-like ground excitation. *Earthq. Eng. Struct. Dyn.* **43**(10), 1463–1481 (2014)
7. Andreaus, U.: Sliding-uplifting response of rigid blocks to base excitation. *Earthq. Eng. Struct. Dyn.* **19**(8), 1181–1196 (1990)
8. Shenton, H.W., Jones, N.P.: Base excitation of rigid bodies. I: formulation. *J. Eng. Mech.* **117**(10), 2286–2306 (1991)
9. Di Egidio, A., Zulli, D., Contento, A.: Comparison between the seismic response of 2D and 3D models of rigid blocks. *Earthq. Eng. Eng. Vib.* **13**, 151–162 (2014)
10. Di Egidio, A., Alaggio, R., Contento, A., Tursini, M., Della Loggia, E.: Experimental characterization of the overturning of three-dimensional square based rigid block. *Int. J. Non-Linear Mech.* **69**, 137–145 (2015)
11. DeJong, M.J., Dimitrakopoulos, E.G.: Dynamically equivalent rocking structures. *Earthq. Eng. Struct. Dyn.* **43**(10), 1543–1563 (2014)
12. Makris, N., Zhang, J.: Rocking response of anchored blocks under pulse-type motions. *J. Eng. Mech.* **127**(5), 484–493 (2001)
13. Dimitrakopoulos, E.G., DeJong, M.J.: Overturning of retrofitted rocking structures under pulse-type excitations. *J. Eng. Mech.* **138**, 963–972 (2012). *Eng. Struct.* **32**, 3028–3039 (2010)
14. Contento, A., Di Egidio, A.: On the use of base isolation for the protection of rigid bodies placed on a multi-storey frame under seismic excitation. *Eng. Struct.* **62–63**, 1–10 (2014)
15. Vassiliou, M.F., Makris, N.: Analysis of the rocking response of rigid blocks standing free on a seismically isolated base. *Earthq. Eng. Struct. Dyn.* **41**(2), 177–196 (2012)
16. Collini, L., Garziera, R., Riabova, K., Munitsyna, M., Tasora, A.: Oscillations control of rocking-block-type buildings by the addition of a tuned pendulum. *Shock Vib.* (2016). <https://doi.org/10.1155/2016/8570538>
17. Brzeski, P., Kapitaniak, T., Perlikowski, P.: The use of tuned mass absorber to prevent overturning of the rigid block during earthquake. *Int. J. Struct. Stab. Dyn.* (2016). <https://doi.org/10.1142/S0219455415500753>
18. de Leo, A., Simoneschi, G., Fabrizio, C., Di Egidio, A.: On the use of a pendulum as mass damper to control the rocking motion of a non-symmetric rigid block. *Meccanica* **51**, 2727–2740 (2016)
19. Di Egidio, A., de Leo, A.M., Contento, A.: The use of a pendulum dynamic mass absorber to protect a Trilithic symmetric system from the overturning. *Math. Problems Eng.* **2019**, Article ID 4843738 (2019). <https://doi.org/10.1155/2019/4843738>
20. Simoneschi, G., de Leo, A.M., Di Egidio, A.: Effectiveness of oscillating mass damper system in the protection of rigid blocks under impulsive excitation. *Eng. Struct.* **137**, 285–295 (2017)
21. Simoneschi, G., Geniola, A., de Leo, A., Di Egidio, A.: On the seismic performances of rigid blocks coupled with an oscillating mass working as TMD. *Earthq. Eng. Struct. Dyn.* **46**, 1453–1469 (2017)

22. Di Egidio, A., de Leo, A., Simoneschi, G.: Effectiveness of mass-damper dynamic absorber on rocking block under one-sine pulse ground motion. *Int. Limits Non-Linear Mech.* (2016). <https://doi.org/10.1016/j.ijnonlinmec.2017.10.015>
23. Ceravolo, R., Pecorelli, M.L., Fragonara, L.Z.: Semi-active control of the rocking motion of monolithic art objects. *J. Sound Vib.* **374**, 1–16 (2016)
24. Di Egidio, A., Simoneschi, G., Olivieri, C., de Leo, A.M.: Protection of slender rigid blocks from the overturning by using an active control system. In: *Proceedings of the XXIII Conference the Italian Association of Theoretical and Applied Mechanics, Salerno, 4–7 September 2017* (2017)
25. Simoneschi, G., Olivieri, C., de Leo, A.M., Di Egidio, A.: Pole placement method to control the rocking motion of rigid blocks. *Eng. Struct.* **167**, 39–47 (2018)
26. Aghagholizadeh, M., Makris, N.: Earthquake response analysis of yielding structures coupled with vertically restrained rocking walls. *Earthq. Eng. Struct. Dyn.* **47**(15), 2965–2984 (2018)
27. Di Egidio, A., Pagliaro, S., Fabrizio, C., de Leo, A.M.: Dynamic response of a linear two d.o.f system visco-elastically coupled with a rigid block. *Coupled Syst. Mech.* **8**(4), 351–375 (2019)
28. Fabrizio, C., Di Egidio, A., de Leo, A.M.: Top disconnection versus base disconnection in structures subjected to harmonic base excitation. *Eng. Struct.* **152**, 660–670 (2017)
29. Fabrizio, C., de Leo, A.M., Di Egidio, A.: Tuned mass damper and base isolation: a unitary approach for the seismic protection of conventional frame structures. *J. Eng. Mech.* **145**(4) (2019). [https://doi.org/10.1061/\(ASCE\)EM.1943-7889.0001581](https://doi.org/10.1061/(ASCE)EM.1943-7889.0001581)